Supporting Information

Subtly tuning intermolecular hydrogen bonds in hybrid crystals to achieve ultrahigh-temperature molecular ferroelastic

Hui Ye, Xiao-Xian Chen, De-Xuan Liu, Bing-Qing Zhao, Yao-Bin Li, Ying Zeng, Wei-Xiong Zhang,* and Xiao-Ming Chen

MOE Key Laboratory of Bioinorganic and Synthetic Chemistry, School of Chemistry, Sun Yat-Sen University, Guangzhou 510275, China. E-mail: zhangwx6@mail.sysu.edu.cn

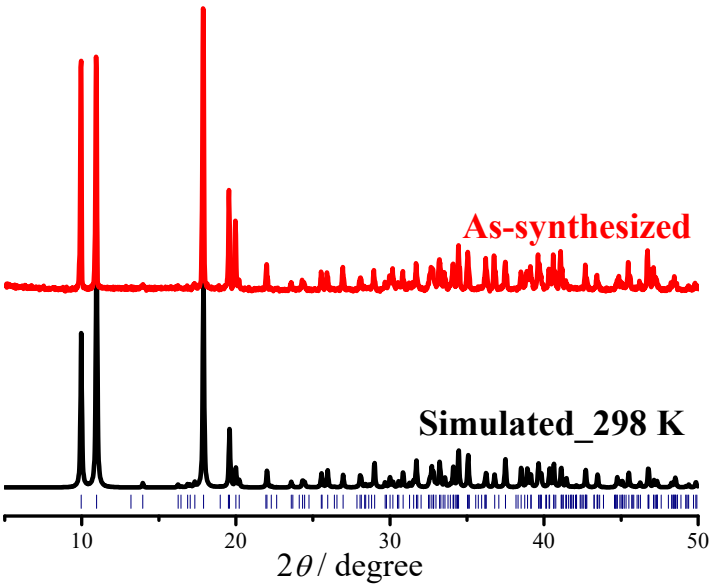

Fig. S1 Simulated (black) and experimental (red) PXRD patterns of **1** at 298 K.

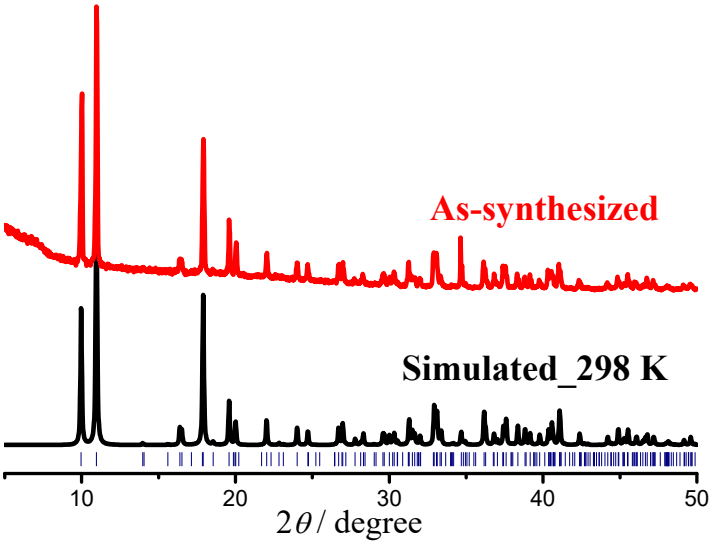

Fig. S2 Simulated (black) and experimental (red) PXRD patterns of **2** at 298 K.

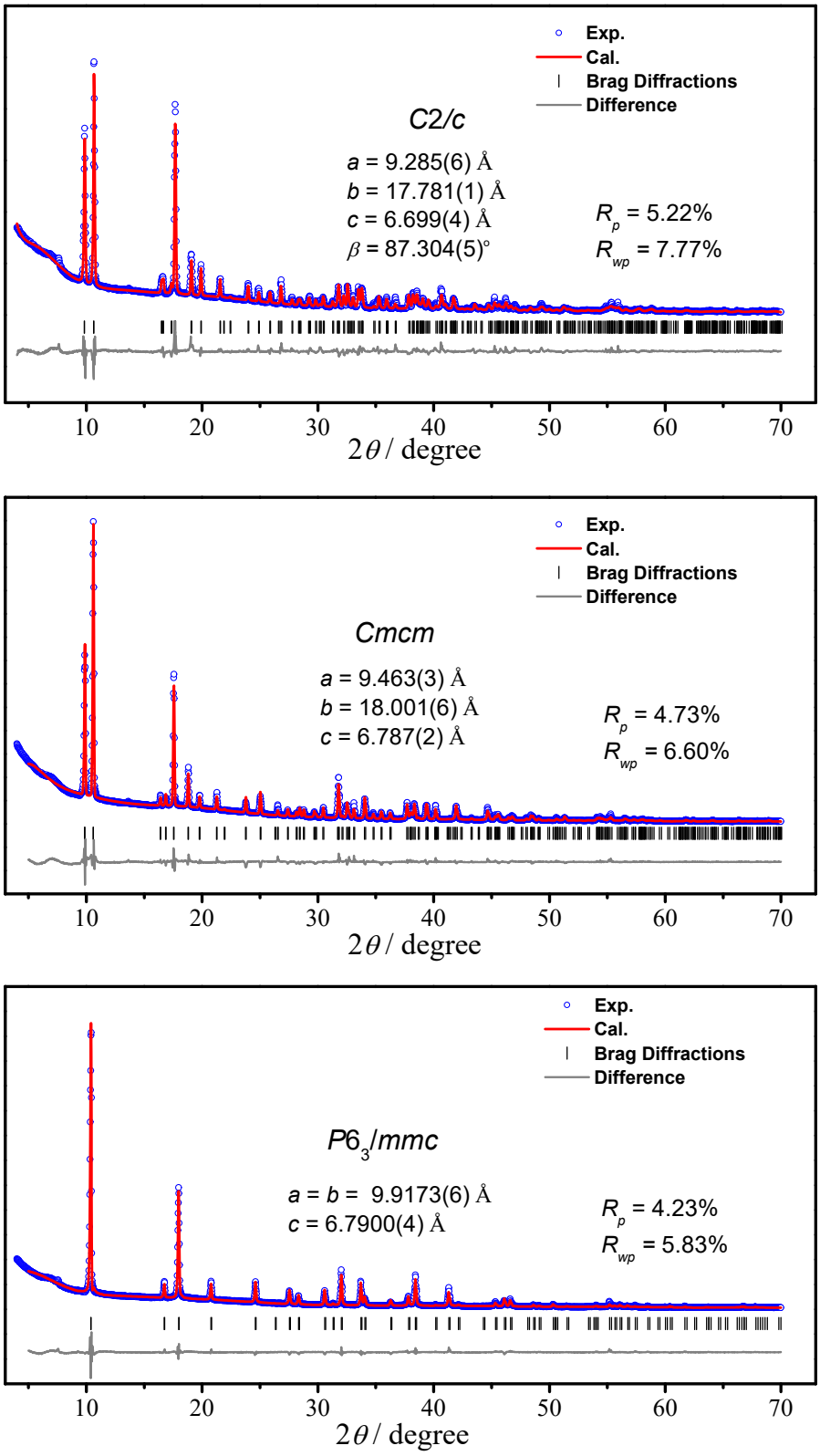

Fig. S3 Final Rietveld refinement results for **2β**, **2γ**, and **2δ** phases, respectively.

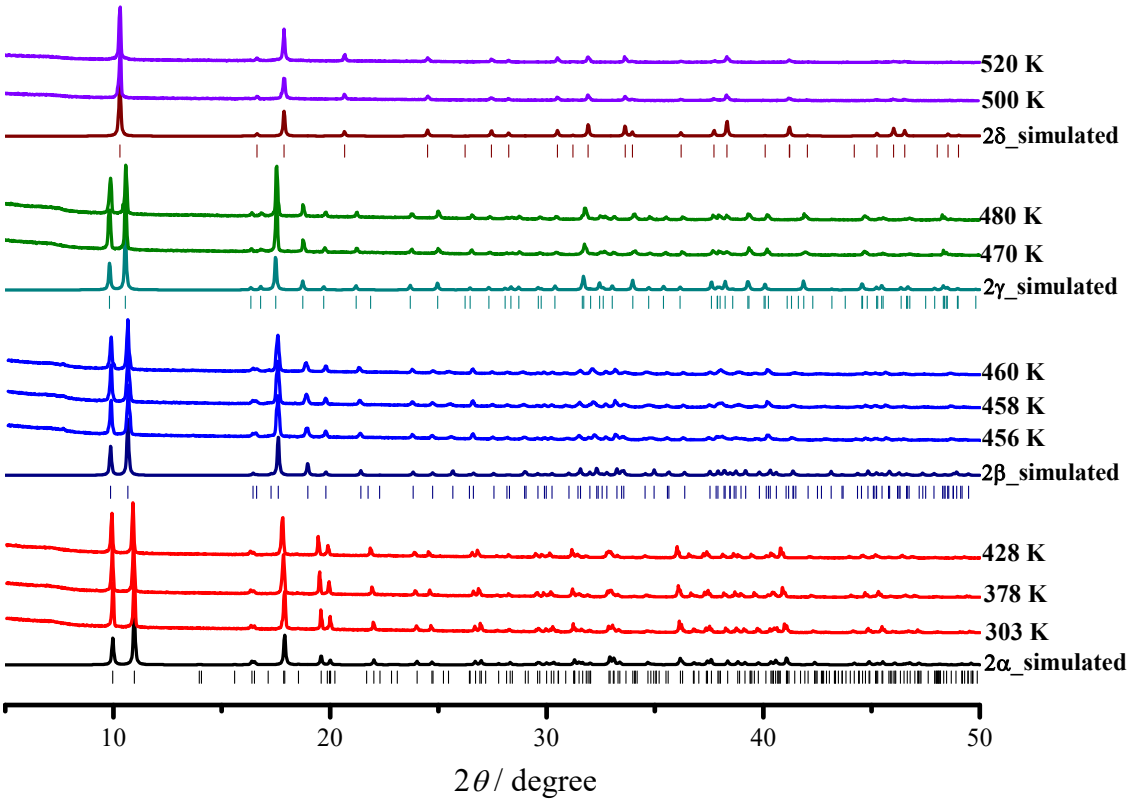

Fig. S4 Variable-temperature experimental PXRD patterns of **2** and the simulated patterns based on the crystal structures of **2α**, **2β**, **2γ**, and **2δ** phases.

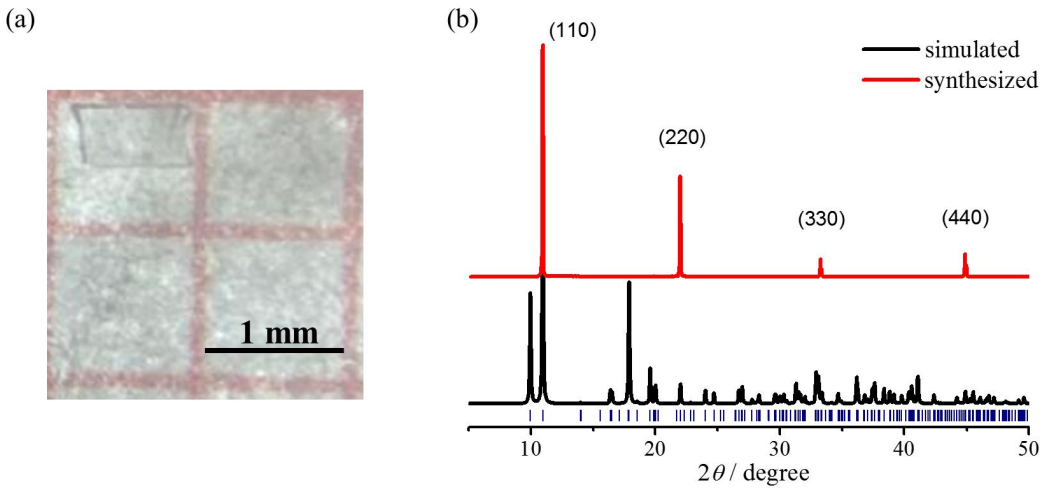

Fig. S5 (a) Morphology of the single crystal of **2** for observation of ferroelastic domains; (b) The simulated PXRD pattern (black) and experiment one (red) measured on the largest plane of single crystal at room temperature.

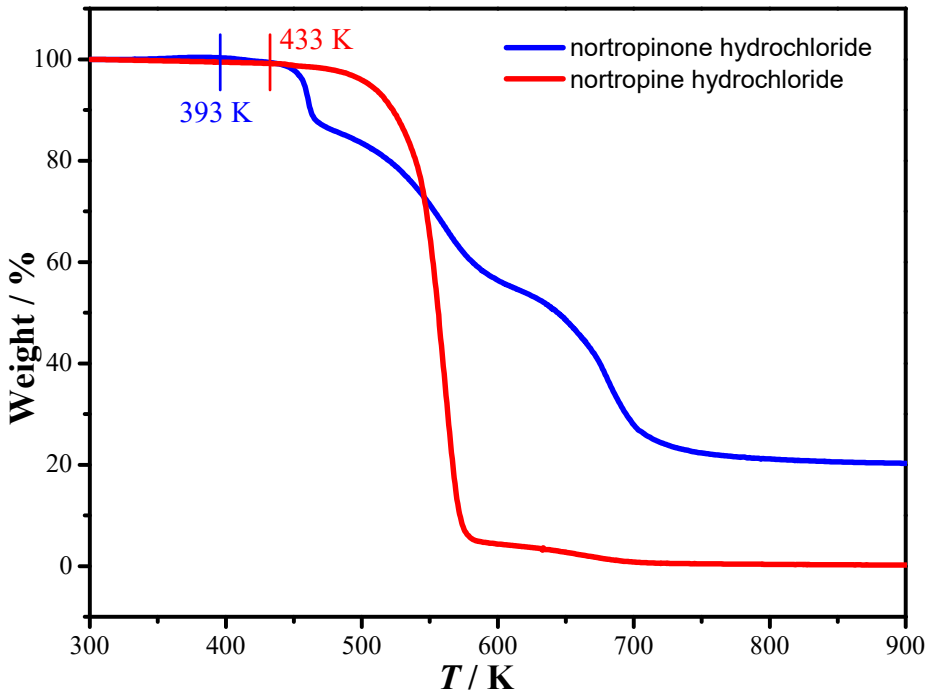

Fig. S6 TGA of nortropinone hydrochloride (blue) and nortropine hydrochloride (red).

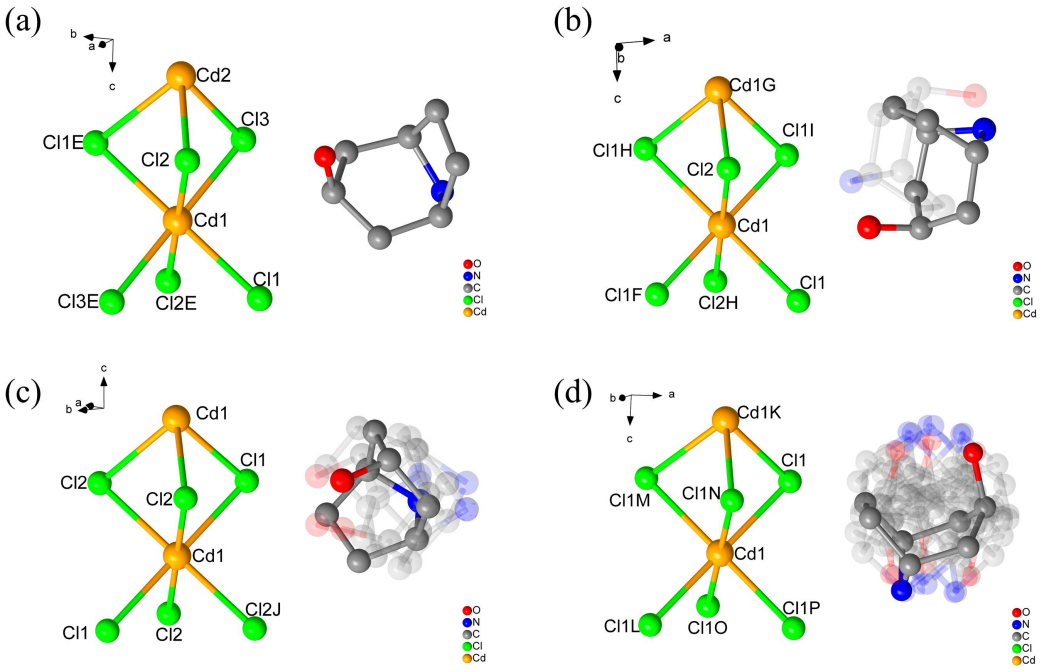

Fig. S7 The asymmetric units of **2α** (a), **2β** (b), **2γ** (c), and **2δ** (d) phases. Symmetric codes: E) -1-*x*, 2-*y*, 2-*z*; F) -*x*, *y*, 3/2-*z*; G) -*x*, *y*, 1/2-*z*; H) -*x*, 1-*y*, 1-*z*; I) *x*, 1-*y*, -1/2+*z*; J) 1-*x*, 1-*y*, -1/2+*z*; K) *x*-*y*, *x*, -1/2+*z*; L)-*x*, -*y*, 1/2+*z*; M) –*x*+*y*, -*x*, *z*; N) -*y*, *x*-*y*, *z*; O) *y*, –*x*+*y*, 1/2+*z*; P) *x*-*y*, *x*, 1/2+*z*. Hydrogen atoms are omitted for clarity.

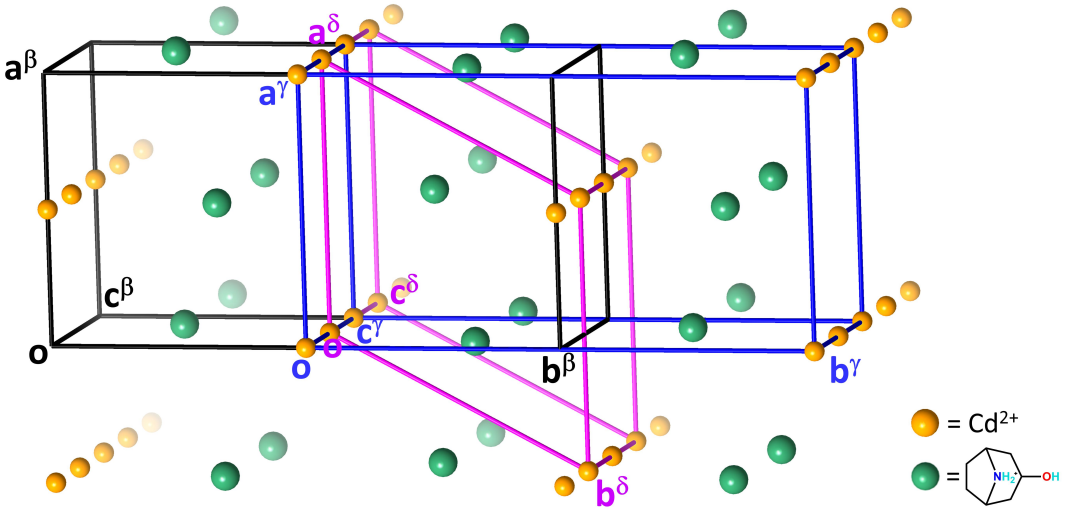

Fig. S8 Relationship between the unit cells in the **2β**, **2γ**, and **2δ** phases. For clarity, only the Cd atoms are drawn based on the crystal structure of **2γ** phase and the $Hntp^{+}$ cations are represented as green balls.

Table S1. Phase-transition temperatures (T_c) and calculated spontaneous strains (ε_{ss}) for different types of perovskites.

Compounds	T_c / K	ε_{ss}	Ferroelastic species	Coordination structure	Ref.
[(*R*)-N-fluoroethyl-3-quinuclidinol][$PbBr_3$]	498	/	622F222	1-D	S1
(nortropinium)[CdCl3]	495 463	0.061 0.018	6/*mmm*F*mmm* *mmm*F2/*m*	1-D	This work
(H_2hpz)[$K(BF_4)_3$]	457	0.0459	*m*3*m*F*mmm*	3-D	S2
$(DMTBA)_3Bi_2Br_9$	425	/	6/*mmm*F*mmm*	1-D	S3
(*R*-CTA)$_2CuCl_4$	417	/	432F32	0-D	S4
[$Fe(Cp)_2$][$FeCl_4$]	407.7	0.1088	$m\bar{3}m$F*mmm*	0-D	S5
($Me_3NCH_2Br)_2$[$ZnBr_4$]	387	0.048	*mmm*F2/*m*	0-D	S6
($C_7H_{17}NBr$)[$Cd(SCN)_3$]	367.8	0.043	6/*mmm*F*mmm*	0-D	S7
($Me_3NCH_2CH_2OH)_4$[$Ni(NCS)_6$]	269 360	0.603 0.0073	4/*mmm*F2/*m* 4/*mmm*F*mmm*	0-D	S8
($Me_4P)_4$[$Mn(SCN)_6$]	352	0.102	*mmm*F2/*m*	0-D	S9
($Me_3NOH)_2$[$ZnCl_4$]	351	0.129	*mmm*F2/*m*	0-D	S10
[CPtmp][$Cd(SCN)_3$]	335 349	0.011 0.011	*mmm*F2/*m* 6/*mmm*F*mmm*	1-D	S11
[Me_3PCH_2OH][$CdBr_3$]	339	0.065	6/*mmm*F*mmm*	1-D	S12
($C_7H_{17}NCl$)[$Cd(SCN)_3$]	335.1	0.054	6/*mmm*F*mmm*	1-D	S7
($C_7H_{13}NH_3)_2$[SnI_4]	319	0.134	*mmm*F2/*m*	2-D	S13
(Me_3PCH_2F)[$Cd(SCN)_3$]	318	0.086	*mmm*F2/*m*	1-D	S14
(MedabcoF)$Rb(BF_4)_3$	309.9 231.3	/	*m*3*m*F4/*mmm* 4/*mmm*F2/*m*	3-D	S15
(Me_4P)[$Cd(SCN)_3$]	308	0.062	*mmm*F2/*m*	1-D	S14
($C_7H_{17}NF$)[$Cd(SCN)_3$]	295.9	0.078	6/*mmm*F*mmm*	1-D	S7
($C_5H_{12}N)_2$[$KBiCl_6$]	285	0.0615	2/*m*$\bar{1}$	1-D	S16
($C_5N_2H_{16})_2$[$SbBr_5$]	278.3	0.355	*mmm*F2/*m*	1-D	S17
($C_3H_5NH_3)_2$[$CdCl_4$]	273	0.239	*mmm*F2/*m*	2-D	S18
(($CH_2)_3NH_2$)[$Mn(HCOO)_3$]	272	0.022	*mmm*F2/*m*	3-D	S19
($C_5H_{12}N)_2$[$CdCl_3$]	254	0.040	*mmm*F2/*m*	1-D	S20

H_2hpz^{2+} = homopiperazine-1,4-diium; $DMTBA^+$ = *N,N*-dimethyl-*tert*-butylaminium;

R-CTA^+ = *R*-3-chloro-2-hydroxypropyltrimethylammonium; $Fe(Cp)_2^+$ = ferrocenium;

$CPtmp^+$ = cyclopentyltrimethylphosphonium;

$MedabcoF^{2+}$ = 1-fluoro-4-methyl-1,4-diazoniabicyclo[2.2.2]octane.

Table S2. Pawley refinement results on the variable-temperature PXRD patterns of **1**

Temperature / K	*a* / Å	*b* / Å	*c* / Å	*V* / Å^3	R_p / %	R_{wp} / %
303	18.598(2)	8.932(1)	6.707(1)	1048.70(1)	5.17	8.66
328	18.609(2)	8.943(1)	6.712(1)	1051.55(1)	5.46	9.04
353	18.623(2)	8.958(1)	6.713(1)	1054.13(1)	5.71	9.29
378	18.630(2)	8.970(1)	6.714(1)	1056.21(1)	5.82	9.53
403	18.641(1)	8.983(1)	6.714(1)	1058.42(1)	5.87	9.50
428	18.653(2)	8.996(1)	6.718(1)	1061.22(1)	5.80	9.48
453	18.662(2)	9.011(1)	6.725(1)	1064.67(1)	5.94	9.76

Table S3. Pawley refinement results on the variable-temperature PXRD patterns of **2**.

Phase	Temperature / K	*a* / Å	*b* / Å	*c* / Å	*V* / Å^3	R_p / %	R_{wp} / %
2α	307	9.047(1)	17.631(1)	6.726(1)	1067.75(1)	3.77	5.12
	328	9.066(1)	17.665(1)	6.733(1)	1073.11(1)	3.84	5.15
	353	9.093(1)	17.710(1)	6.742(1)	1080.58(1)	3.82	5.11
	373	9.120(1)	17.755(1)	6.750(1)	1087.66(1)	3.86	5.10
	398	9.150(1)	17.796(1)	6.758(1)	1095.26(1)	3.84	5.18
	428	9.196(1)	17.861(1)	6.769(1)	1106.89(1)	4.11	5.49
2β	453	9.324(1)	17.825(1)	6.716(1)	1115.31(1)	4.73	6.27
	455	9.334(1)	17.825(1)	6.717(1)	1116.72(1)	4.55	6.16
	457	9.343(1)	17.825(1)	6.717(1)	1117.90(1)	4.93	6.58
2γ	470	9.378(1)	17.831(1)	6.730(1)	1125.38(1)	4.26	5.90
	475	9.400(1)	17.842(1)	6.735(1)	1129.56(1)	4.20	5.72
	480	9.412(1)	17.852(1)	6.743(1)	1132.98(1)	4.11	5.47
	485	9.436(1)	17.867(1)	6.750(1)	1138.00(1)	4.26	5.64
	490	9.451(1)	17.874(1)	6.760(1)	1141.95(1)	4.39	5.96
			$\sqrt{3}b$ / Å				
2δ	500	9.894(1)	17.137(1)	6.775(1)	1148.72(1)	4.27	5.76
	505	9.901(1)	17.149(1)	6.781(1)	1151.36(1)	4.27	5.64
	510	9.907(1)	17.159(1)	6.784(1)	1153.24(1)	4.16	5.63
	515	9.915(1)	17.173(1)	6.787(1)	1155.62(1)	4.12	5.54
	520	9.921(1)	17.184(1)	6.792(1)	1157.92(1)	4.13	5.51

Table S4. Thermal expansion coefficients of the principle axes in **1**.

	Temperature / K	Principle axis	Direction			α / MK^{-1}	β_v / MK^{-1}
			a	*b*	*c*		
1	303–453 K	X_1	-0.0092	-0.0000	1.0000	15(2)	97(3)
		X_2	0.7078	0.0000	0.7065	23(1)	
		X_3	-0.0000	1.0000	-0.0000	59 (1)	

Table S5. Thermal expansion coefficients of the principle axes in **2**.

	Temperature / K	Principle axis	Direction			α / MK^{-1}	β_v / MK^{-1}
			a	*b*	*c*		
2α	307–428 K	X_1	0.0031	-0.0000	1.0000	52(1)	305(9)
		X_2	0.0000	-1.0000	0.0000	108(2)	
		X_3	0.9921	0.0000	0.1251	140(7)	
2β	453–457 K	X_1	0.4563	-0.0000	0.8898	-492(6)	585(9)
		X_2	0.0000	-1.0000	0.0000	6(1)	
		X_3	-0.7018	0.0000	0.7124	1071(14)	
2γ	470–490 K	X_1	0.0000	-1.0000	0.0000	125(4)	740(8)
		X_2	0.0000	0.0000	1.0000	223(13)	
		X_3	1.0000	0.0000	-0.0000	388(9)	
2δ	500–520 K	X_1	0.0000	1.0000	-0.0000	122(3)	395(6)
		X_2	-1.0000	-0.0000	0.0000	137(1)	
		X_3	0.0000	0.0000	1.0000	134(4)	

Table S6. Liner fitting results of variable-temperature cell parameters of **2**.

Phase	Fitting equations	R^2	Deduced parameters at T_{c2} (463 K)	Deduced parameters at T_{c3} (495 K)
2α	$a = 0.00123T + 8.66319$	0.991		
	$b = 0.0019T + 17.04226$	0.997		
	$c = 0.000357T + 6.61628$	0.999		
2β	$a = 0.00475T + 7.17242$	0.998	9.371 Å	
	$b = 0.0000975T + 17.78042$	0.965	17.825 Å	
	$c = 0.000095T + 6.67341$	0.889	6.717 Å	
	$\beta = 0.08475T + 49.30942$	0.998	88.55°	
			V = 1104.93 Å^3	
2γ	$a = 0.00364T + 7.6682$	0.989	9.354 Å	9.47 Å
	$b = 0.00222T + 16.7876$	0.989	17.815 Å	17.887 Å
	$c = 0.0015T + 6.0236$	0.984	6.718 Å	6.766 Å
			V =1119.50 Å^3	V = 1146.10 Å^3
2δ	$a = 0.00136T + 9.214$	0.997		9.887 Å
	$b = 0.00236T + 15.9568$	0.997		17.125 Å
	$c = 0.0008T + 6.3758$	0.977		6.772 Å
				V = 1146.60Å^3

Table S7. Ferroelastic species and phase-transition temperatures (T_c) for reported dual ferroelastics.

Compounds	Space groups	Point groups	T_c's / K	Ref.
(nortropinium)[$CdCl_3$]	*C*2/*c*-*Cmcm*-*P*6$_3$/*mmc*	2/*m*-*mmm*-6/*mmm*	463, 495	This work
($Me_3NCH_2CH_2OH$)$_4$[$Ni(NCS)_6$]	*P*2$_1$/*n*-*P*4/*mnc*-*Bmab*	2/*m*-4/*mmm*-*mmm*	269, 360	S8
[CPtmp][$Cd(SCN)_3$]	*P*2$_1$/*c*-*Cmcm*-*P*6$_3$/*mmc*	2/*m*-*mmm*-6/*mmm*	335, 349	S11
(MedabcoF)Rb(BF_4)$_3$	*P*2$_1$/*c*-*P*4$_2$/*mbc*-*Fm*$\bar{3}$*c*	2/*m*-4/*mmm*-*m*$\bar{3}$*m*	231, 310	S15

Table S8. Hydrogen-bond distances and angles for **1**

D	H	A	*d* (D-H) / Å	*d* (H-A) / Å	*d* (D-A) / Å	D-H-A / º
N1	H1A	Cl3	0.89	2.43	3.301(3)	166.5
N1	H1B	O1A	0.89	2.02	2.855(4)	155

Symmetric code for **1**: A) *x*, *y*, -1+*z*.

Table S9. Hydrogen-bond distances and angles for **2α**.

D	H	A	*d* (D-H) / Å	*d* (H-A) / Å	*d* (D-A) / Å	D-H-A / º
O1	H1	Cl1D	0.82	2.44	3.244(2)	168.8
N1	H1A	Cl1Q	0.89	2.75	3.435(3)	134.3
N1	H1B	O1C	0.89	2.06	2.941(4)	169.6

Symmetric codes for **2**: C) -1/2+*x*, 3/2-*y*, 1/2+*z*; D) 1/2+*x*, 3/2-*y*, -1/2+*z*; Q) -1/2+*x*, 3/2-*y*, -1/2+*z*.

The equations for calculation of the spontaneous strain.

The spontaneous strain tensors can be given as:

$$\varepsilon_{ij} = \begin{bmatrix} \frac{a_{\beta\ phase}}{a_{\gamma\ phase}} - 1 & 0 & \frac{c_{\beta\ phase}}{2c_{\gamma\ phase}}\cos\beta \\ 0 & \frac{b_{\beta\ phase}}{b_{\gamma\ phase}} - 1 & 0 \\ \frac{c_{\beta\ phase}}{2c_{\gamma\ phase}}\cos\beta & 0 & \frac{c_{\beta\ phase}}{c_{\gamma\ phase}}\sin\beta - 1 \end{bmatrix} = 0.018$$

for *mmm*F2/*m*, and

$$\varepsilon_{ij} = \begin{bmatrix} \frac{a_{\gamma\ phase}}{a_{\delta\ phase}} - 1 & 0 & 0 \\ 0 & \frac{b_{\gamma\ phase}'}{b_{\delta\ phase}} - 1 & 0 \\ 0 & 0 & \frac{c_{\gamma\ phase}}{c_{\delta\ phase}} - 1 \end{bmatrix} = 0.061$$

for 6/*mmm*F*mmm*, based on a necessary conversion of lattice parameters, where *b* phase'= *b* phase /$\sqrt{3}$.

The detail for determining space groups for 2β, 2γ, and 2δ.

To solve the crystal structures for **2β**, **2γ**, and **2δ**, respectively, we carefully analyzed their PXRD patterns by using the Reflex module of Material Studio 5.0, meanwhile taking account of the chemical rationality during the phase transitions. The general process is: 1) Indexing the experimental PXRD pattern to get the possible unit cells and corresponding crystal class; 2) Carrying out an initial pawley refinement by using the candidate unit cells in the lowest-symmetric space group possible for the given crystal class (to exclude system extinction possible); 3) Listing the possible space groups by using the automatic space group determination in Materials Studio, and then carefully excluding some space groups by comprehensively considering R factor, figure of merit, the chemical rationality (such as chirality and centrosymmetry), and the mismatch between the experimental peaks and simulated ones (*vide infra*); 4) Carrying out pawley refinement(s) again by using the rest candidate unit cell(s) in the possible space group(s) and carefully check the resulted *R* factor(s) and the match(es) between the experimental and simulated peaks; 5) Built the initial structural model(s) in the candidate unit cell(s) by taking account of the chemical rationality, and submit it to the Rietveld refinement(s); 6) Stepwise optimizing the parameters until the Rietveld refinement converge, and comprehensively evaluating the results based on *R* factors, the agreement between simulated and experimental powder patterns, as well as the chemical rationality.

For **2β**, seven candidate space groups were recommended by using the automatic space group determination: *Cn*, *Cc*, *C*2/*c*, *C*2/*n*, *C*2/*m*, *Cm*, and *C*2. Among them, four polar or chiral space groups (*Cn*, *Cc*, *Cm*, and *C*2) could be excluded in considering that 2α belongs to centrosymmetric space group ($P2_1/n$) without disordered molecular components hence should transform to centrosymmetric space group upon heating. As shown in figure S9, the pawley refinements based on *C*2/*n* and *C*2/*m* cells showed thatsome experimental peaks do not match the simulated Bragg positions, while the experimental pattern well agree with simulated one with obviously reduced R_p and R_{wp} values based on *C*2/*c* unit cell. Therefore, the *C*2/*c* unit cell was choose as

the most possible cell, and was further confirmed by the the successes of following model building and Rietveld refinement (Figure S3).

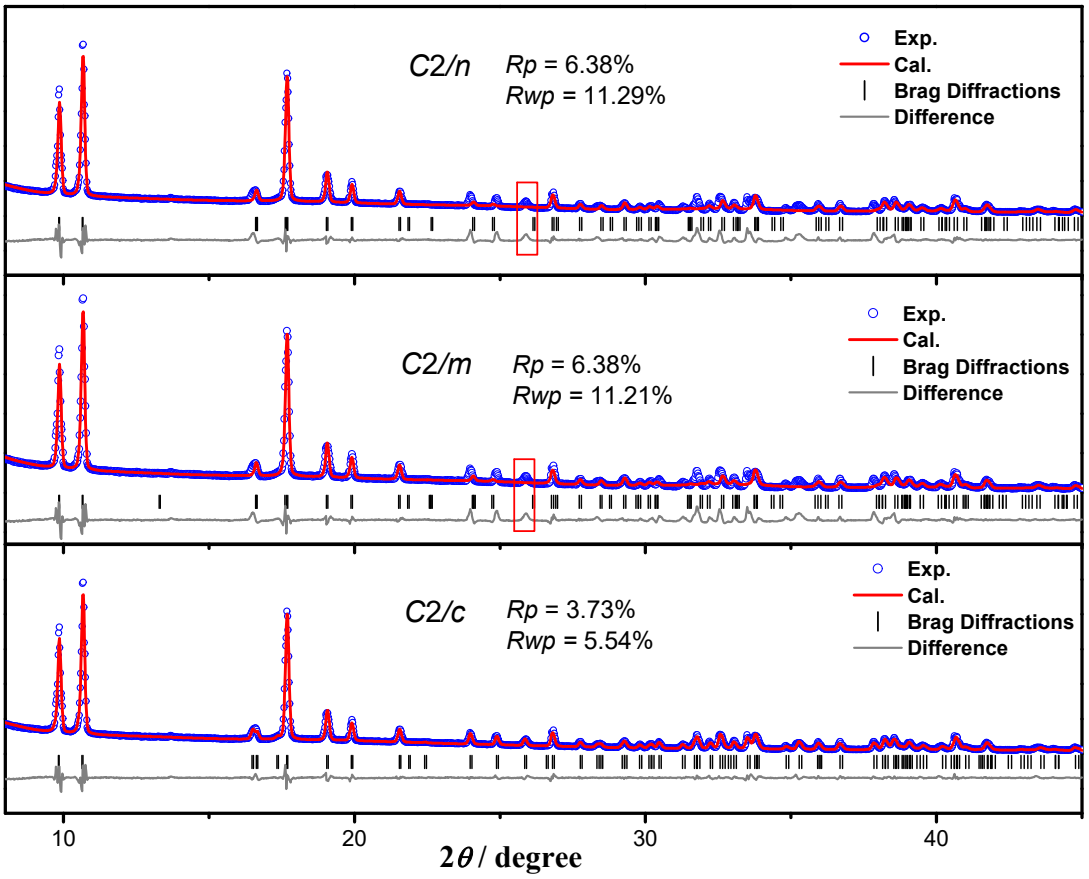

Figure S9. Pawley refinements based on *C*2/*n*, *C*2/*m*, and *C*2/*c* unit cell, respectively.

Similarly, for **2γ**, only *Cmcm* and *Cccm* are centrosymmetric space groups among the candidate space groups recommended by using the automatic space group determination. As illustrated in Figure S10, two experimental diffraction peaks obviously do not indexed by the *Cccm* unit cell, while the entire experimental PXRD pattern agree well with the simulated one based on *Cmcm* unit cell. Therefore, the most possible space group for **2γ** is *Cmcm*, and was further confirmed by the the successes of following model building and Rietveld refinement (Figure S3).

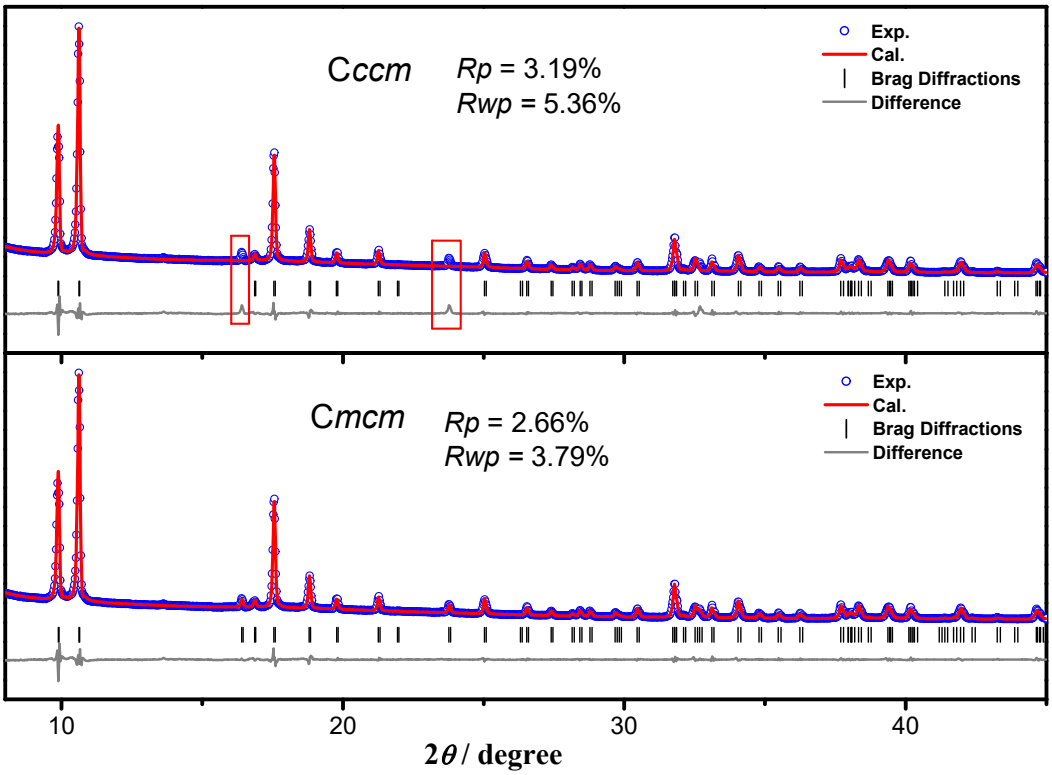

Figure S10. Pawley refinements based on *Cccm* and *Cmcm* unit cell, respectively.

For **2δ**, the ideal $P6_3/mmc$ prototype of hexagonal perovskite was choose as the first option in considering that the organic cations could be highly disordered in **2δ**. In addition, given the orthorhombic crystal class in **2γ**, the **2δ** should belong to point group 6/*mmm* to yield a ferroelastic **2δ→2γ** transition observed by variable-temperature polarization microscopy (Figure 7b), while $P6_3/mmc$ is the only one belonging to the point group 6/*mmm* among the candidate space groups recommended by using the automatic space group determination. Therefore, the most possible space group for **2δ** is $P6_3/mmc$, and was further confirmed by the successes of Pawley refinement (Figure S11) and Rietveld refinement (Figure S3) showing well agreements between the experimental PXRD pattern and the simulated one.

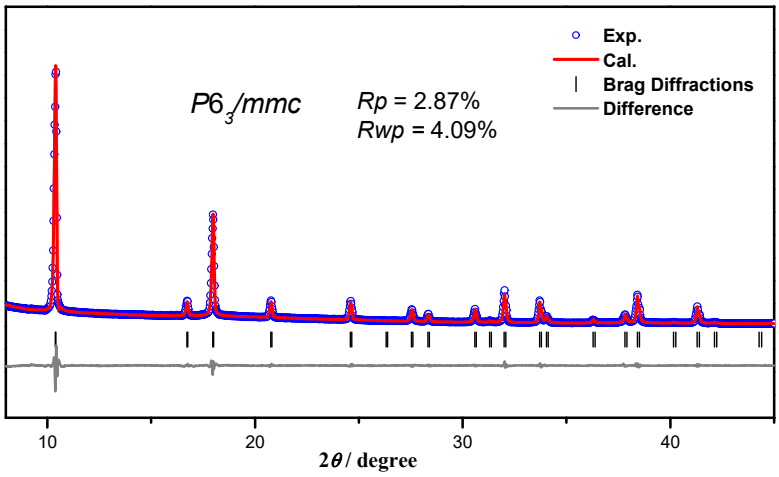

Figure 11. Pawley refinement results based on $P6_3/mmc$ unit cell.

In addition, the space groups $P2_1/n$, $C2/c$, and *Cmcm* are typical subgroups of $P6_3/mmc$ and commonly observed in the known hexagonal perovskite crystals, and such a space group change ($P2_1/n$-$C2/c$-*Cmcm*-$P6_3/mmc$) is well agree with the observed domain revolution by the variable-temperature polarization microscopy (Figure 7). Therefore, we believe that $C2/c$, *Cmcm*, $P6_3/mmc$ are the most possible space group for **2β**, **2γ**, and **2δ**, respectively, after carefully excluding some space group by considering the chemical rationality, pattern agreement, and *R* factor.

Reference

S1. Y.-Y. He, Z. Chen, X.-G. Chen, X.-M. Zhang and D.-Y. Fu, *Mater. Chem. Front.*, 2022, DOI: 10.1039/D2QM00058J.

S2. X.-X. Chen, X.-Y. Zhang, D.-X. Liu, R.-K. Huang, S.-S. Wang, L.-Q. Xiong, W.-X. Zhang and X.-M. Chen, *Chem. Sci.*, 2021, **12**, 8713.

S3. Z.-X. Zhang, C.-Y. Su, J. Li, X.-J. Song, D.-W. Fu and Y. Zhang, *Chem. Mater.,* 2021, **33**, 5790-5799.

S4. S.-Q. Lu, Z.-X. Zhang, H. Cheng, P.-F. Li, W.-Q. Liao and R.-G. Xiong, *Angew. Chem., Int. Ed.*, 2020, **59**, 9574-9578.

S5. H.-Y. Zhang, C.-L. Hu, Z.-B. Hu, J.-G. Mao, Y. Song and R.-G Xiong, *J. Am. Chem. Soc.*, 2020, **142**, 3240-3245.

S6. J.-X. Gao, X.-N. Hua, P.-F. Li, X.-G. Chen and W.-Q. Liao, *J. Phys. Chem. C*, 2018, **122**, 23111-23116.

S7. L. He, L. Zhou, P.-P. Shi, Q. Ye and D.-W. Fu, *Chem. Mater.*, 2019, **31**, 10236-10242.

S8. D.-X. Liu, X.-X. Chen, Z.-M. Ye, W.-X. Zhang and X.-M. Chen, *Sci. China Mater.*, 2022, **65**, 263-267.

S9. Q. Li, P.-P. Shi, Q. Ye, H.-T. Wang, D.-H. Wu, H.-Y. Ye, D.-W. Fu and Y. Zhang, *Inorg. Chem.*, 2015, **54**, 10642-10647.

S10. W. Yuan, Y. Zeng, Y.-Y. Tan, J.-H. Zhou, W.-J. Xu, W.-X. Zhang and X.-M. Chen, *Chem. Commun.*, 2019, **55**, 8983–8986.

S11. L. Zhou, R.-X. Li, P.-P. Shi, Q. Ye and D.-W. Fu, *Inorg. Chem.*, 2020, **59**, 18174-18180.

S12. X. Zheng, L. Zhou, P.-P. Shi, F.-J. Geng, D.-W. Fu and Q. Ye, *Chem. Commun.*, 2017, **53**, 7756-7759.

S13. X.-N. Li, P.-F. Li, Z.-X. Wang, P.-P. Shi, Y.-Y. Tang and H.-Y. Ye, *Polyhedron*, 2017, **129**, 92-96.

S14. Y.-J. Cao, L. Zhou, P.-P .Shi, Q. Ye and D.-W. Fu, *Chem. Commun.*, 2019, **55**, 8418-8421.

S15. S.-N. Cheng, K. Ding, T. Zhang, Z.-X. Zhang, C.-Y. Su, J.-Z. Ge, Y. Zhang and D.-W. Fu, *Chem. Eur. J.*, 2021, **27**, 17655-17659.

S16. Q.-R. Meng, W.-J. Xu, W.-H. Hu, H. Ye, X.-X. Chen, W. Yuan, W.-X. Zhang and X.-M. Chen, *Chem. Commun.*, 2021, **57**, 6292.

S17. C.-Y. Mao, W.-Q. Liao, Z.-X. Wang, Z. Zafar, P.-F. Li, X.-H. Lv and D.-W. Fu, *Inorg. Chem.*, 2016, **55**, 7661-7666.

S18. S.-G Han, X.-T. Liu, J. Zhang, C.-M. Ji, Z.-Y. Wu, K.-W. Tao, Y.-Y Wang, Z.-H. Sun and J.-H. Luo, *J. Mater. Chem. C*, 2018, **6**, 10327-10331.

S19. W. Li, Z.-Y. Zhang, E. G. Bithell, A. S. Batsanov, P. T. Barton, P. J. Saines, P. Jain, C. J. Howard, M. A. Carpenter and A. K. Cheetham, *Acta Materialia Inc.*, 2013, **61**, 4928-4938.

S20. A. Zeb, Z.-H. Sun, T. Khan, M. A. Asghar, Z.-Y. Wu, L.-N. Li, C.-M. Ji and J.-H. Luo, *Inorg. Chem. Front.*, 2017, **4**, 1485-1492.